Mapping Flood Extent Using a Simple DEM-Inundation Model

Tao Zheng¹ and Yong Wang² Central Michigan University¹ Easr Carolina University²

A grid-based one-dimensional digital elevation model (DEM)-inundation model has been developed as a tool for flood extent mapping on floodplains. The validity and accuracy of the model have been assessed through comparison of modeled results with those derived from the widely used standard and complex 1-D Hydrologic Engineering Center–River Analysis System (HEC-RAS) model and verification against the September 1999 flood on the lower Tar River floodplain, North Carolina. The two models are comparable in accuracy. With its simple implementation and ease of parameterization, the DEM-inundation model is a potential alternative to the HEC-RAS model.

Introduction

Floods are one of the most significant natural hazards, costing lives, serious damage to property, and disruptions to social and economic activities. The ability to map the flood extent accurately and timely can provide critical information for immediate flood relief activities, and pre- and post- flood mitigation efforts (Mileti 1999, Colby et al. 2000, Yang and Tsai 2000, Al-Sabhan et al. 2003). To this end, hydraulic models have been developed and used for mapping flood extent (Hydraulic Engineering Center 1997, Correia et al. 1998, Ackerman et al. 2000, Chang et al. 2000, Dobson and Li 2000, Al-Sabhan et al. 2003, Hunter et al. 2005, Bates et al. 2006). Over the years, both two- and onedimensional hydraulic models have been developed. The 2-D models include those that employ sophisticated full finite-element approaches or that take grid-based approaches. For instance, Galland et al. (1991) developed a 2-D finite element numerical model, the TELEMAC-2D. Nicholas and Mitchell (2003) also developed a finite-element 2-D model that solves the depthaveraged shallow water form of the Navier-Stokes equations. The 2-D models are generally capable of achieving high mapping accuracy, especially for hydraulic processes at fine spatial resolution, but they require digital elevation models (DEMs) of high resolution and accuracy, as well as other geophysical model inputs. They all are computationally intensive. To avoid the drawbacks of the finite-element models, Bates and De Roo (2000) developed a raster-based model, the LISFLOOD-FP, which takes a storage cell approach to simulate flood hydrologic and hydraulic process. The LISFLOOD-FP has been subsequently improved and validated for the January 1995 flooding on the River Meuse, the Netherlands (Hunter et al. 2005, Bates et al. 2006).

Unlike 2-D models, 1-D hydraulic models are typically characterized by a series of cross-sections of channel and floodplain topography. Validation tests have reported that 1-D models, such as the Hydraulic Engineering Center-River Analysis System (HEC-RAS), are capable of reaching high accuracy in flood extent mapping (Horritt and Bates 2002). Investigations have been also conducted on how the accuracy of the model can be affected by various factors, such as mesh resolution, topographic representation, and spatial resolution (Horritt and Bates 2001, Horritt et al. 2006).

In short, the existing 1-D and 2-D models can map a flood extent accurately, but they are difficult to be parameterized. Among others,

the estimation of Manning's coefficient of friction as input to the models, which is also referred to as Manning's n (Chow 1959), is highly uncertain and unreliable. For instance, laboratory experiments have reported higher values for Manning's n than those recommended in the well-established tables by V. T. Chow in 1959 (Wilson and Horritt 2002). Although different values have been recommended (Acrement and Schneider 1989) and extensive studies have been conducted to derive the coefficients (Werner et al. 2005, Wilson et al. 2006), there is still no proven way to estimate the n with a high level of confidence and accuracy. Additionally, the implementation of the existing models requires advanced levels of hydrologic and hydraulic knowledge and expertise, which is often lacking among prospective users, therefore hindering the use of the models. Thus, there are clear needs for a hydraulic model that is simple in parameterization and implementation. Such a simple model, if capable of reaching comparable accuracy of the complex model, can serve as an alternative. In addition, a simple model can provide initial and preliminary analysis, and the result can help the complex model for indepth study.

To meet the needs for simple flood-extent mapping models, Wang et al. (2002) developed a model that maps flood extent by linearly interpolating the surface water height of a river between two neighboring gauging stations using the heights measured at the stations. In this article, an improved version of Wang et al. (2002)'s model is developed. The newly developed model is a 1-D DEM-inundation model that features three major improvements. First, Wang et al. (2002)'s model did not identify the central channel of the river; this model does. Second, Wang et al. (2002) represented distance between gauging stations with a straight line, whereas this model traces the distance along the central channel line between two neighboring gauging stations. Lastly, the changes in elevation of a river channel and banks along a river, which are important geometric factors affecting a river's water surface height at different flow conditions, were not modeled (Wang et al. 2002). This

DEM-inundation model accounts for these factors in the water surface height interpolation. In summary, the objectives of this paper are to detail the development of a DEM-inundation model, to compare the model with the HEC-RAS model to assess their accuracy in flood extent mapping, and to validate the DEM-inundation model against a real flood event.

Methodogy: HEC-RAS Model

To meet the needs for flood extent mapping, the Hydraulic Engineering Center (HEC) of the US Army Corps of Engineers developed a series of GIS-based hydraulic models, from the Arc/HEC2 to HEC-RAS (Hydrologic Engineering Center 1997, Kraus 2000, Ackerman et al. 2000, USACE 2007). HEC-RAS is one of the most popular 1-D hydraulic models. Compared with its predecessors, HEC-RAS comes with some major improvements. It facilitates the use of digital datasets such as DEM and TIN (triangular irregular network) (Correia et al. 1998, Dobson and Li 2000, Yang and Tsai 2000), and features an enhanced graphical user interface that simplifies the flood extent modeling processes.

The HEC-RAS model is designed to perform 1-D hydraulic calculation for a full network of natural or constructed water channels. In the model, surface profiles of a steady flow in which changes in flow depth and velocity occur gradually over a considerable length of channel are solved by using a 1-D energy equation and energy head loss equation (Hydraulic Engineering Center 1997). The steady flow's water surface profiles are computed from downstream to upstream at cross sections for a given discharge rate at upstream and water surface height value at downstream. In the solving of the water surface profile along a river channel, HEC-RAS requires geometric and hydraulic input parameters. The geometric parameters include the river system schematics, cross section profile, reach length, energy loss coefficient, and stream junction information. The schematic parameters define how river reaches are connected. Cross section profiles are required at locations where changes in discharge, slope, shape, and roughness occur along the river channel between the up- and down- stream. The reach length refers to the measured distance between cross sections. The reach lengths for the left overbank, right overbank, and channel are required. To evaluate energy losses, HEC-RAS uses energy loss coefficients including a) Manning's *n* value for friction loss (Chow 1959), b) contraction and expansion coefficients to evaluate transition loss, and c) bridge and culvert loss coefficients to evaluate losses related to weir shape, pier configuration, pressure flow, and entrance and exit conditions. The hydraulic inputs include flow regime, peak discharge information, and boundary conditions that include known water surface elevation, critical depth, normal depth, and rating curve.

Methodology: One Dimensional DEM-inundation Model

Compared with the complex HEC-RAS model, the 1-D DEM-inundation model calculates an artificial water height surface using surface water height of a stream and compares the artificial surface with the DEM to determine water/non-water or flooded/ non-flooded areas. The surface water height measurements are available at gauging stations. Because the distance between two neighboring gauging stations may be quite large, surface water heights between stations must be interpolated to create the artificial water height surface. This is accomplished in four major steps, the delineation of the stream centerline, derivation of surface water height along the centerline, estimation of the reach of the centerline's surface water height for locations off the centerline, and finally creation of the surface water height grid for different flow conditions. To delineate the centerline of a river section, we

- a) Overlay co-located aerial photographs or remotely sensed images over the DEM covering the stream section in question. Then, a tentative centerline is drawn in such a way that it is positioned approximately equidistant between the left and right banks.
- b) Identify the first DEM pixel on the upstream

end of the tentative centerline, and use it as the center for searching the pixel with lowest elevation value within a certain radius. Our experiment indicated that a radius of 300 m is sufficient for most cases, which is equivalent of 10 pixels on 30 x 30 m USGS DEM. This pixel with the lowest elevation is then the actual location of the delineated centerline. Move one pixel downstream along the tentative centerline, and perform the similar searching until the downstream end of the tentative centerline is reached. Thus a lowest-elevation pixel is identified for each corresponding pixel on the centerline.

c) Manually draw a new centerline by tracing through all the pixels with the lowest-elevation values from the upstream to downstream ends. d) Verify the centerline created in the step 3 with the DEM, aerial photographs or satellite images. If needed, repeat steps a), b), and c) until a satisfactory result is achieved. A satisfactory centerline should be continuous with each pixel positioned at the lowest point of its corresponding cross-section.

Typically, the delineated centerline is a curved line composed of the deepest pixels along a river stream.

Second, the water surface height at each location or pixel along the centerline is calculated. An assumption used for this calculation is that water surface height decreases from upstream to downstream and that the decrease depends on the changes of location and elevation long the centerline. Figure 1 illustrates the calculation. Let A be the upstream end and B the downstream end where the channel's elevations (E_A and E_B) on river's centerline and surface water height (H_A and H_B) are known. Let X be a location between A and B. At X, elevation (E_X) is derived from DEM and water surface height (H_X) is computed using

$$\begin{cases} H_{x} = H_{A} \\ If \Delta E \cdot \Delta D = 0 \quad and E_{X} + D_{X} = 0 \end{cases}$$

$$\begin{cases} H_{x} = H_{A} - \Delta H \cdot \frac{E_{X}D_{X}}{E_{X} + D_{X}} \left(\frac{1}{\Delta E} + \frac{1}{\Delta D} \right) \\ If \Delta E \cdot \Delta D \neq 0 \quad or E_{X} + D_{X} \neq 0 \end{cases}$$

$$(1)$$

where H_A = water surface height at location A,

 ΔH = water surface height difference between gauging stations A and B,

 ΔE = elevation difference between A and B,

 ΔD = distance between A and B along the stream centerline,

 $H_{\rm X}$ = water surface height at point X, $E_{\rm X}$ = stream channel's elevation at location X, and

 D_X = distance between A and X along the stream centerline.

In general, one should select locations $\mathcal A$ and $\mathcal B$ where gauging stations are located. Thus, $\mathcal H_{\mathcal A}$ and $\mathcal H_{\mathcal B}$ as well as $E_{\mathcal A}$ and $E_{\mathcal B}$ are known.

Third, with water surface heights at each pixel along the centerline calculated, one is ready to compute water heights at pixels off the centerline. With the assumption that water surface at a cross section is level, calculation of the surface water height at an off-centerline pixel is boiled down to finding the oncenterline pixel to which the off-centerline pixel shares a same cross-section. This is achieved by finding the on-centerline pixel with shortest straight line distance to the off-centerline pixel in question. There are four steps involved in this procedure:

a) Identify all the on-centerline pixels that are within a specified radius of the off-centerline pixel.

b) Calculate the straight line distance between the off-centerline pixel and each on-centerline pixel using the equation:

D = $((x_e - x_p)^2 + (y_e - y_p)^2)^{0.5}$ (2) where x_e and y_e are x and y coordinates of pixel C, x_p and y_p are x and y coordinates of pixel P_i , i = 1, 2, 3, ..., n and represents the series of oncenterline pixels that lie within the search radius (Figure 2). The x and y coordinates are relative to the origin located at the lower left corner of the study area as covered by the DEM, assuming the DEM used is of a square or rectangular shape.

c) Identify the on-centerline pixel *C* that has the shortest straight line distance to the off-centerline pixel.

d) Assign the surface water height to the off-

centerline pixel according to the assumption of level water surface at stream cross-sections.

e) Repeat the process for all off-centerline pixels. (Note: A C program was written to accomplish this step.)

Lastly, once all of the surface water heights are calculated, both on-centerline and off-centerline, a surface water height layer (a grid) is created with same spatial resolution as underlying DEM. It should be pointed out that if the size of the search radius for the nearest on-centerline pixel to offline-pixel is difficult to determine, searching the entire study area could be an alternative; it can, however, be very time consuming. There are other methods available for interpolating water surface height based on known water surface height at nearest points. For example, Werner (2001) used the inverse distance weighted interpolation.

Methodology: Modeling Flood Extents by Using DEM-inundation and HEC-RAS Models

In the delineation of the flood extent, the 1-D DEM-inundation model superimposes the calculated surface water height layer over the DEM layer. Because both layers are grids with the same spatial resolution, the values of surface water height and ground elevation at each pixel are known. To delineate water/non-water (regular flow) or flooded/non-flooded (flood flow) areas, one needs to have two sets of a stream's surface water heights (a regular one and a flood one). Thus, two surfaces of the water heights are calculated. At a location X, let $H_{X-regular}$ be the regular height and $H_{X-flood}$ be the flooded height on the two surfaces, respectively. Then,

- · if a location's elevation (on the DEM data) is $\leq H_{X-regular}$, then the location is classified as regular stream area,
- · if its elevation is > $H_{X\text{-regular}}$ and $\leq H_{X\text{-flood}}$ then the location is a flooded area, or
- · if the elevation is $> H_{X,flood}$, then the location is non-flooded or dry.

The HEC-RAS model simulation with regular and flood river surface height will also classify

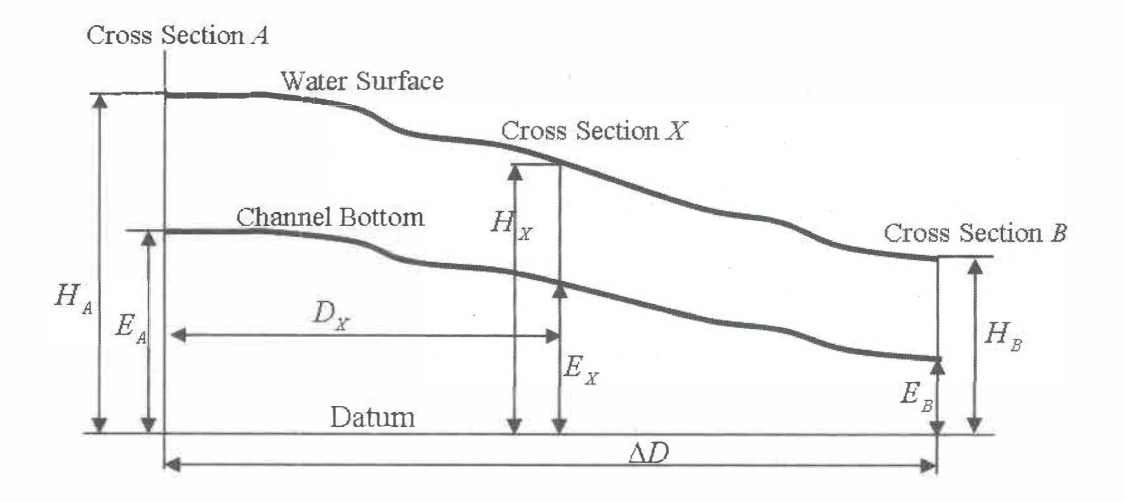


Figure 1. Illustration of the interpolation of water surface height, H_{X_i} at a given location X on the stream centerline.

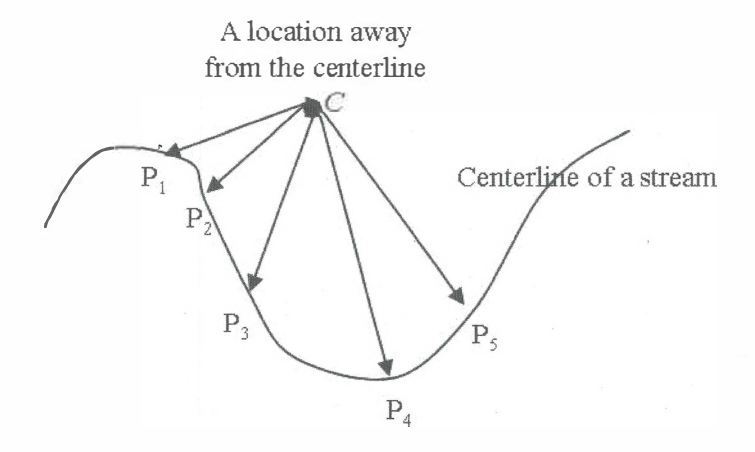


Figure 2. Interpolation of water surface height for an off-centerline location, C. Five points, $P_{i_1}P_{i_2}P_{i_3}P_{i_4}$ and P_{i_5} on the central channel are shown as an example. Distances between C and all points on the channel are calculated, so that the point(s) on the centerline having the shortest distance to C will be identified.

each pixel within the study area as regular stream, flooded, or dry (non-flooded).

Methodology: Comparison and accuracy assessment of flood extents derived by both models

To compare the inundation extents from both models, first we summarize descriptive statistics of the regular stream area, flooded area, and non-flooded area. Next, spatial comparison analysis of the extents at the same flow condition is carried out to quantify the amount of agreement between the two models on a pixel-by-pixel basis. If a pixel is classified as same category (regular stream, flooded, or non-flooded area) by the two models, there is an agreement; otherwise, there is a disagreement.

The water/non-water or flooded/non-flooded boundaries delineated by the DEM-inundation and HEC-RAS models can differ so to understand the variation of the boundaries statistically, we used the matched-pair t-test of the boundaries on both sides of the river channel. Figure 3 shows two sets of boundaries, one centerline, and nine channel crosssections. (The centerline is depicted as straight line for simplicity.) Neighboring cross-sections are roughly 400 m apart in this study. Along each crosssection, two interception points with the boundaries are obtained; the distances between the two points and the centerline are calculated. Once the distance measurements for all cross-sections are computed, there are two sets of distance measurements: one from the DEM-inundation model and the other from the HEC-RAS model. The null hypothesis (H_o) for the t-test is that there is no difference between the distances from the two models (i.e., the boundaries are statistically identical), and the alternative hypothesis (H₄) is that a significant difference exists between the two models. A significant level of $\alpha = 0.05$ is chosen to test whether H_a should be rejected. Similarly, distance measurements and t-test was be carried out for the boundaries on the other side of the centerline (e.g., Figure 3).

Finally, to validate the 1-D DEM-inundation model as well as HEC-RAS model, we evaluated modeled flood extents at a record-high flood flow

on 23 September 1999 against remotely sensed data and *in situ* measurements obtained at several sites. The date and site selection are based on available ancillary datasets detailed in the next section. Error matrices are used to quantify the mapping accuracy

Methodology: Study Area and Datasets

The study area is on the lower floodplain of the Tar/Pamlico River (drainage area ~ 157 km²), North Carolina. It covers part of Pitt County on the west and Beaufort County on the east (Figure 4). The Tar River flows into Pitt from the northwest and exits to Beaufort to the east. After passing the bridge of Highway 17, it is called the Pamlico River. There are two USGS gauging stations, one at Greenville and the other at Washington (Figure 4). Greenville is the largest city in Pitt County, and Washington is the largest city in Beaufort County. There are three major reasons for choosing this particular study area: floods triggered by heavy precipitation, tropical storms and hurricanes occur frequently in the study area; the two river gauging stations provide the real-time measurements for water surface height and daily mean discharge; and on-going flood research in this area has resulted in several in-house geo-spatial and remote sensing datasets (Colby et al. 2000, Wang et al. 2002, Wang 2004, Wang and Zheng 2005).

Based on the statewide land use and land cover layer created by the North Carolina Center for Geographic Information and Analysis, there are fifteen land use and land cover types within the study area (Wang 2004). Bottomland forests/hardwood swamps and cultivated areas were dominant land cover types (about 73% of the study area). The bottomland forests/hardwood swamps are areas of deciduous and woody vegetation taller than 3 m, where crown density is at least 25%. Tupelo (N. aquatica) and cypress (Cupressus) are the major species. The cultivated lands are areas occupied by crops of cotton, corn, tobacco, and soybeans. In addition, there are developed areas, which count for about 3% of the study area and are mainly concentrated in the vicinity of the cities

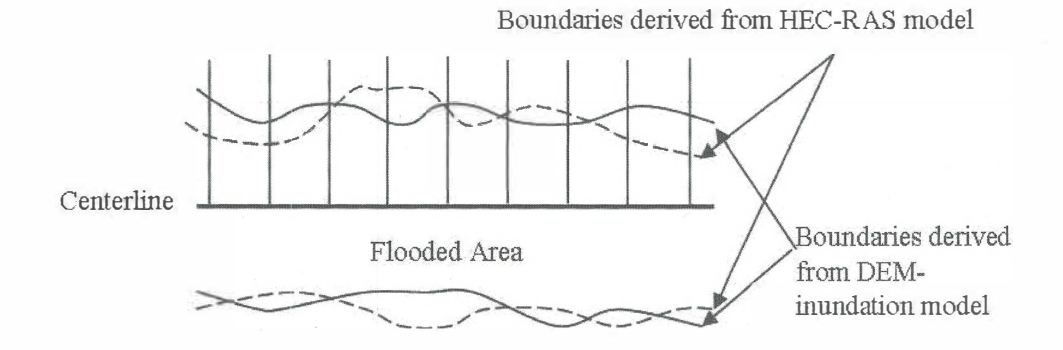


Figure 3. Hypothetical boundaries derived from the HEC-RAS and DEM-inundation models. Nine cross-sections are plotted at evenly-distributed intervals.

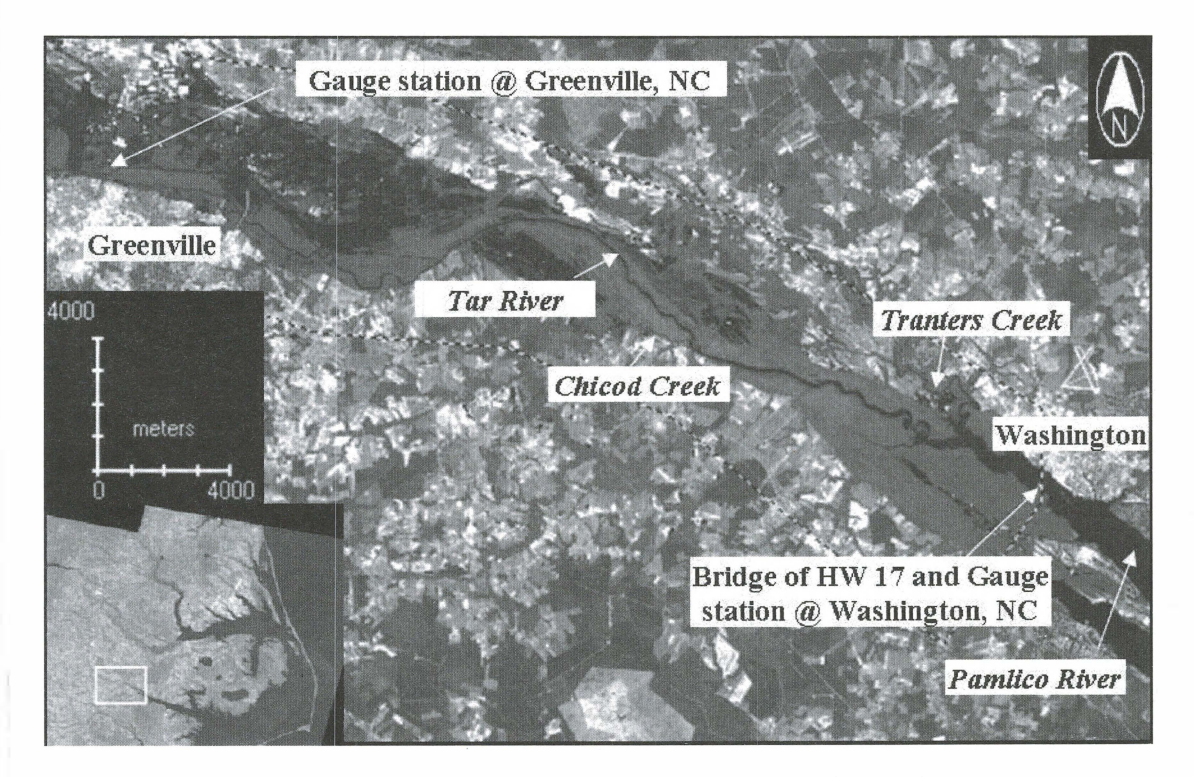


Figure 4. Landsat 7 ETM+ data of band 8 on 23 September 1999 (path/row 14/35). The study area outlined by the dotted lines covers the Tar/Pamlico River floodplain, North Carolina.

of Greenville and Washington (Wang 2004). The statewide land use and land cover data are used to estimate the Manning's n coefficient of roughness at each cross-section along the river channel, which is one of the most important input parameters to the HEC-RAS model.

The surface water height and discharge data collected at the gauging stations of Greenville and Washington are given in Table 1. The DEM-inundation model only uses the water surface height, whereas HEC-RAS model requires both height and discharge along with other previously discussed inputs. Inundation extents are modeled at two representative flooding flow conditions: a flood-stage flow on 28 February 2003 and a record-high flood flow on 23 September 1999. The flow condition on 28 July 1999 is used as the regular flow (because of the availability of Landsat ETM+ data). Thus, comparisons of the modeled results under the two distinct flood-flow situations as referenced to the regular flow condition can be performed.

DEM data for the study area were obtained from the USGS National Elevation Dataset. The DEM has a 30 m by 30 m horizontal spatial resolution and a vertical accuracy of ±1m (USGS NED 2007). The terrain within the study area is flat with a minimum elevation of 0.0 m, a median of 3.5 m, a maximum of 22.5 m, a mean of 4.7 m, and a standard deviation of 4.0 m. Thus, any significant increase of river's surface water height could inundate a large area. Also, it should be noted that the south side of the Tar River has considerably more relief than the north side. Conceivably, the accuracy of DEM has a significant impact on flood mapping and the availability of higher accuracy DEM will improve floodplain modeling assessment. On the other hand, because DEM accuracy should similarly impact both models, the NED DEM is considered as a reasonable choice for comparing the two models under the same set of conditions.

Remotely sensed imagery and aerial photography were used to identify flooded and non-flooded areas to aid the validation of inundation extents resulting from the two models. These datasets include Landsat 7 ETM+ data acquired on 28 July 1999 and 23 September 1999, and oblique aerial photographs

taken on 23 September 1999. These datasets, combined with in situ observations made in October 1999, were used to identify twenty-five flooded sites, twenty-five regular river sites, and twenty-five nonflooded sites. Thus, the accuracy of the modeled flood extents at the record-high flood flow can be evaluated at the seventy-five sites. The areas covered by the sites and by categories are: regular river area of 4.63 km², flooded area of 4.41 km², and nonflooded area of 5.32 km², for a total of 14.36 km² or 9.1% of the entire study area. Since there is no other remotely sensed or in situ datasets on 28 February 2003, no verification of the modeled results were performed. It should be noted that the USGS Digital Orthophoto Quarter (DOQQs) acquired in 1998 were used to aid the initial identification of the steam centerline (on the DEM) and landuse categories for sites where ground access is impossible. Finally, all digital datasets used for this study have been re-projected into the Universal Transverse Mercator (UTM) coordinate system using the World Geodetic System-1984 (WGS84) models for the spheroid and datum.

Results and Discussion

Two layers consisting of water and non-water categories covering the entire study area were first created at the regular river flow condition (Table 1) using DEM-inundation and HEC-RAS models, respectively (Figure 5). In the figure, the water area is shown in black and non-water area in white. The main channel of the Tar River is clearly delineated, and two tributaries (Chicod and Tranters creeks, Figure 5b) are identified. Visual examination of the modeled results indicates that the water areas may be similar. However, in the upstream section there is more area classified as water by the HEC-RAS model than by the DEM-inundation model (Figure 5). At the regular flow, water areas are 11.85 km² and 16.95 km², according to the DEM-inundation model and HEC-RAS model, respectively (Table 2).

Four additional layers were modeled for water and non-water categories for the flood-stage flow and record-high flood flow conditions using the two models. The water areas on all these four layers include the regular river surface area (e.g., Figure 5),

Water height (m)

	Regular	Flood-stage	Record-high
Date	28/07/1999	28/02/2003	23/09/1999
Discharge (m³/s)	4.39 / NA	302.99 / 311.49	1846.26 / 2152.08

3.30 / 0.31

Table 1. River data measured at the Greenville and Washington gauging stations.

Table 2. Modeled extents of regular river, flooded, and non-flooded areas (km²) at three flow conditions.

		Regular	Flooded	Non-flooded
Regular flow	DEM-inundation	11.85	XXX	145.12
	HEC-RAS	16.95	XXX	140.02
Flood-stage flow	DEM-inundation	11.85	56.10	89.02
	HEC-RAS	16.95	45.67	94.35
Record-high	DEM-inundation	11.85	77.80	67.31
	HEC-RAS	16.95	74.35	65.67

which should be excluded in order to map the flooded area. This exclusion is done through recoding and overlaying operations. Thus four inundation maps representing the flood extents when the Tar River was at a flood-stage flow (Figure 6) and at a record-high flood flow (Figure 7) were generated. In these figures, the regular river areas are shown in black, the flooded area in gray and non-flooded area in white.

0.37 / 0.27

At the flood-stage flow on 28 February 2003 (Figure 6), there are large flooded areas surrounding the regular river area, and more flooded areas to the north of the river than to the south. The lower relief on the north bank than south bank is a factor contributing to this difference. Comparison of both inundation maps indicates that more disagreements occur within the upper half of the study area (northwest) than at the lower half (southeast). There are non-flooded islands (surrounded by flooded area). For example, there is an island in the middle of the

flooded area on the inundation map derived from the DEM-inundation model (Figure 6a), and an island of much larger size exists at the corresponding location on the flood map derived from the HEC-RAS model (Figure 6b). Both islands are identified using black arrows in the figures.

7.96 / 1.60

Figure 7 shows the modeled inundation extents at a record-high flood flow condition. The extents are visually similar. The aerial digital photographs acquired on 23 September 1999 and ground truth collected in October 1999 indicate that the majority of flooding occurred on the north side of the river, where the elevation is much lower than the corresponding part on the south side. The slightly higher elevation on the south bank is one major factor to its smaller flooded area as compared to the north side. Two noticeable disagreements of the extents as pointed by two pairs of black arrows are observed: one occurs near the northwest corner and the other near the easternmost location. In addition,

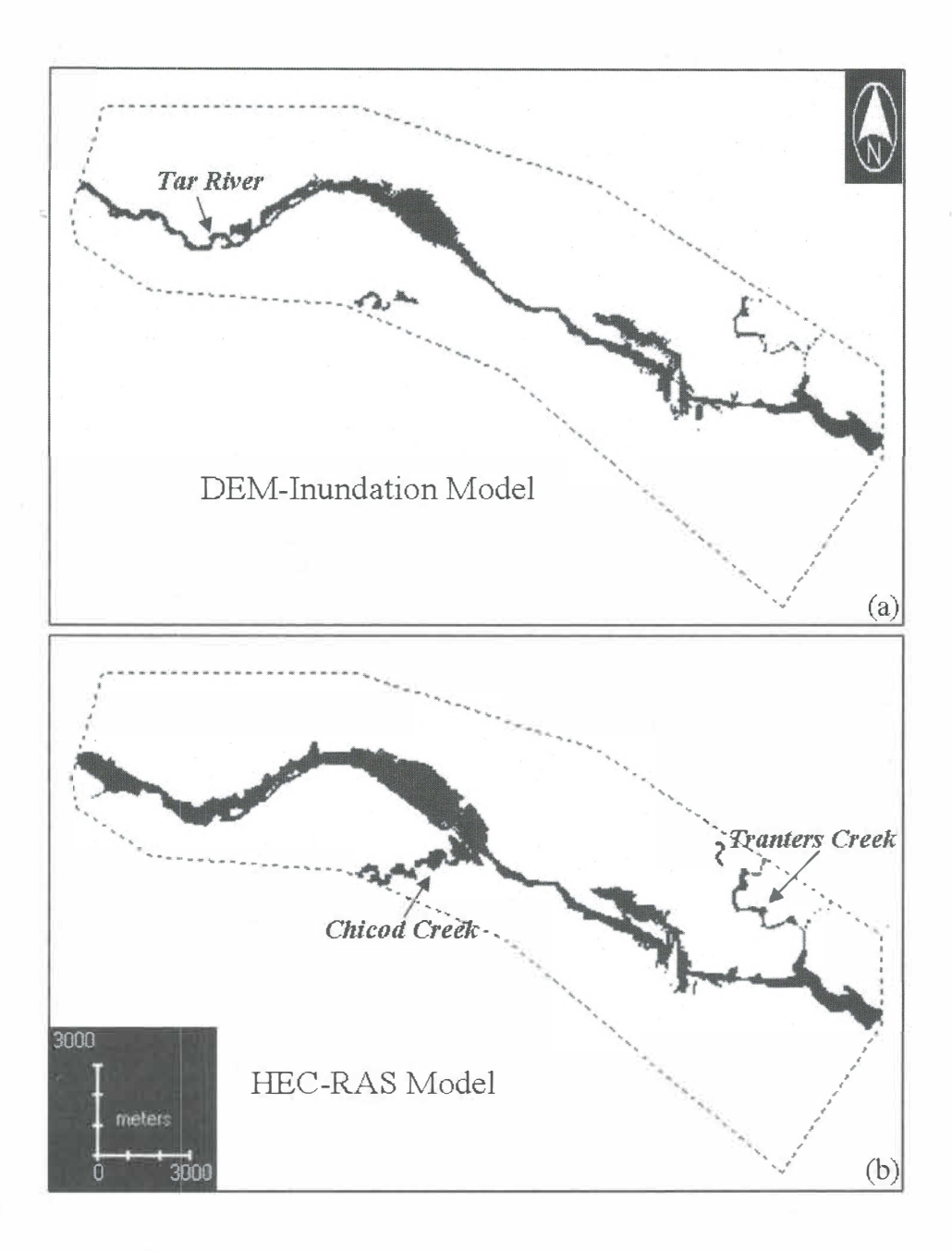


Figure 5. Regular river area (in black) and non-water area (in white) derived from a) DEM-inundation model and b) HEC-RAS model at a regular flow on 28 July 1999.

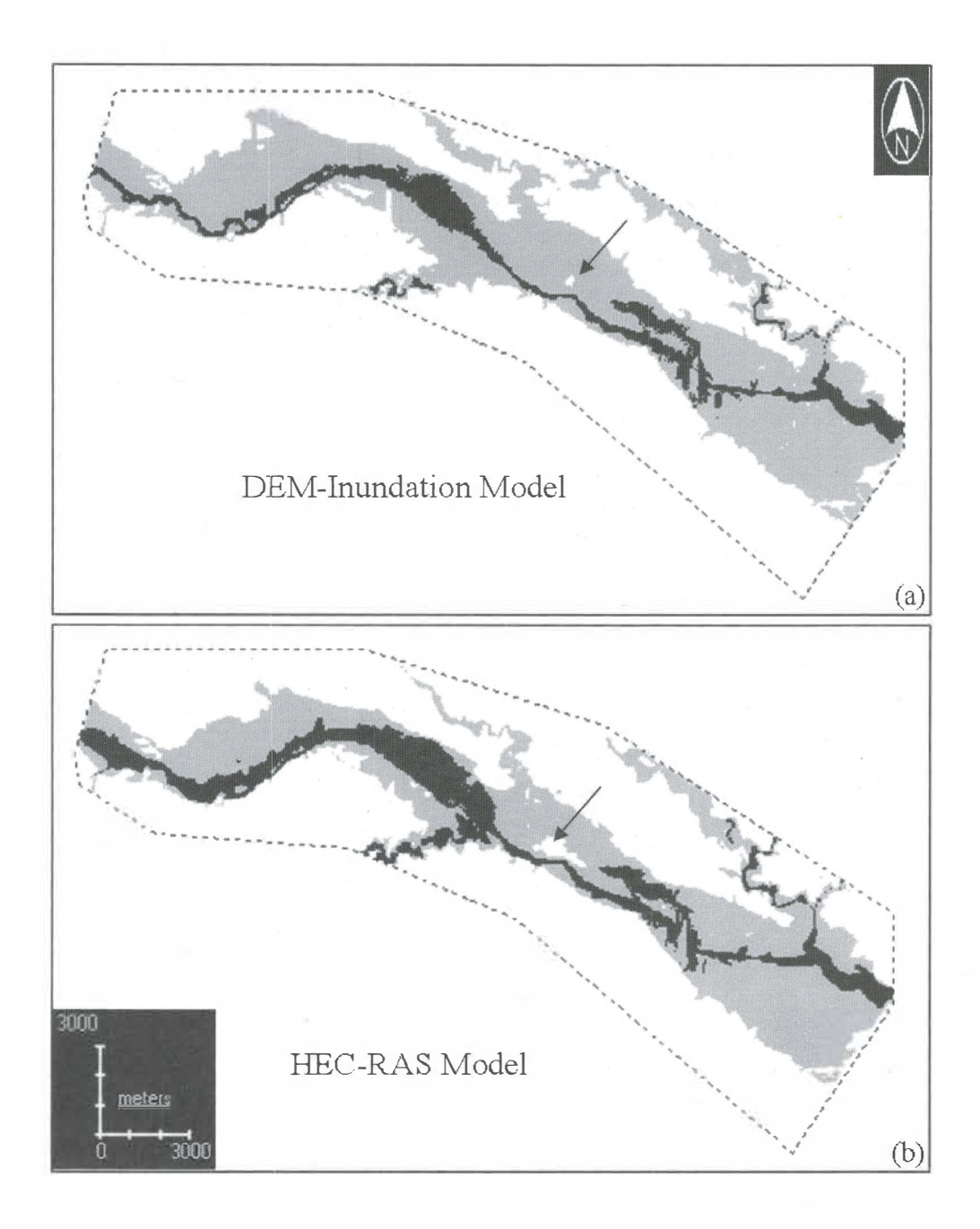


Figure 6. Inundation extents derived from a) the DEM-inundation model and b) the HEC-RAS model at a flood stage flow on 28 February 2003. The regular river area is in black, flooded area in gray, and non-flooded area in white. Unflooded islands exist, as pointed by black arrows as examples.

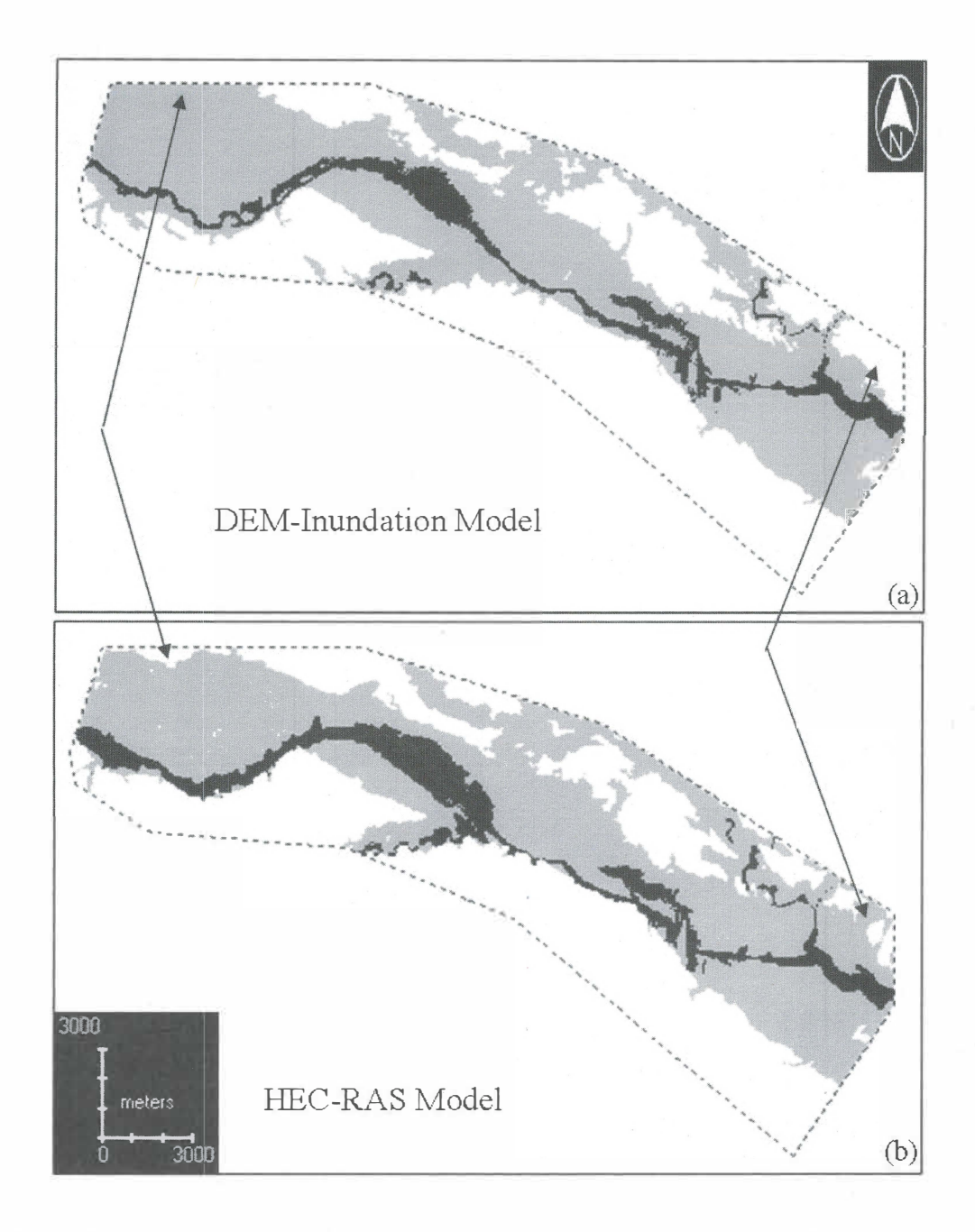


Figure 7. Inundation extents derived from a) DEM-inundation model and b) HEC-RAS model at a record-high flood flow on 23 September 1999.

in comparison with Figure 6, there is much greater flooded area in Figure 7, especially within the upstream section where the majority of non-flooded islands are now flooded. The increased flooded areas are attributed to the higher water surface level and discharge volume on 23 September 1999 compared to 28 February 2003 (Table 1). Table 2 summarizes the area of each category on each inundation extent map. As the river changes from its flood-stage to record-high flood flows, flooded areas increase from 56.10 to 77.80 km² (based on DEM-inundation model) and 45.67 to 74.35 km² (HEC-RAS model).

The spatial comparison analysis of the modeled inundation maps at the same flow condition quantified the degree of agreement on a pixel-by-pixel basis. The area classified as the same categories by the two models is 150.18² km (of a total area of 157 km²) or 95.7% on 28 July 1999 maps, 142.08 km² or 90.5% on the 28 February 2003 maps, and 140.34 km² or 89.4% on 23 September 1999 maps (Table 3). Table 3 also details the agreements and disagreements by the categories.

The results of the *t*-tests on the mean distance from the stream centerline to the water/non-water or flooded/non-flooded boundaries on both banks of the inundation maps are shown in Table 4. On 28 July 1999, t and p values for the water/non-water boundaries are 1.573 and 0.122 for the north bank and 1.633 and 0.109 for the south bank, respectively. The p values at both banks suggest that the null hypotheses are not rejected, indicating that the water/non-water boundaries resulting from the DEM-inundation and HEC-RAS models are not statistically different. Because the p values of the t-tests for the flood-stage flow and record-high flood flow are all greater than or equal to 0.103 (Table 4), we conclude that the flooded/non-flooded boundaries on the north and south banks are statistically the same.

Thus far, the DEM-inundation and HEC-RAS models have comparable results in this study area. The findings are very encouraging. Next, the DEM-inundation model and the HEC-RAS model were put to the final test. The accuracy of the modeled flood extents at the seventy-five selected sites were

validated against the ancillary datasets collected during and after the 1999 flood, as described in the previous sections. The results indicated that both models reached high accuracy (Table 5). Based on the DEM-inundation model, the producer's accuracies are between 88.3% and 99.3% and user's accuracies 93.1% and 94.6%. The overall accuracy is 95.1%. Similar high accuracies are also obtained by using the HEC-RAS model (Table 5).

Conclusion

A hydraulic 1-D DEM-inundation model, which is simpler than the standard complex 1-D HEC-RAS model, has been developed. Compared with the HEC-RAS model, the DEM-inundation model requires fewer input parameters that are readily available. The DEM-inundation model is also easier to implement than the HEC-RAS model. Furthermore, comparisons between inundation extents from the models and accuracy evaluation for a flood event on the floodplain of the Tar/Pamlico River, North Carolina have shown that the results from the two models are very similar and both reached overall accuracy greater than 93%. Thus, the DEM-inundation model can be an effective alternative to the more complex HEC-RAS model.

Before concluding, we would like to mention three recent developments: the creation of the DEM for the state of North Carolina, implementation of more river gauging stations by the USGS, and availability of real-time gauge data. All of these developments positively impact the application of the DEMinundation model. After the 1999 flood in eastern North Carolina, the state of North Carolina initiated a statewide flood mapping program (NC Floodplain Mapping Program 2007). One of the products downloadable for free from the program is the statewide light detection and ranging (LIDAR) derived DEM. The DEM is of 15 x 15 m (50 x 50 ft.) resolution, and has a vertical accuracy of approximately 0.2 m. One distinct feature of the new LIDAR-derived DEM, as compared with other DEMs (e.g., NED DEM), is that the LIDAR-derived DEM has been hydro-corrected, i.e., all the channels of streams

Table 3. Spatial comparison of the inundation extent maps derived from both models at three flow stages. The area is in km², and the percentage within the [] is computed out of the total study area.

(a) A regular flow (07/28/1999)

	Non-water area	Water
DEM-inundation model		
Non-water area	139.17 [88.7%]	5.95 [3.8%]
Water	0.84 [0.5%]	11.01 [7.0%]

(a) A flood-stage flow (02/28/2003)

HEC-RAS model

	TILC-Mis model		
	Non-flooded area	Flooded area	Regular river area
DEM-inundation model			
Non-flooded area	87.94 [56.0%]	1.07 [0.7%]	0.00 [0.0%]
Flooded area	7.02 [4.5%]	43.13 [27.5%]	5.94 [3.8%]
Regular river area	0.04 [0.0%]	0.80 [5.1%]	11.01 [7.0%]

(a) A record-high flood flow (09/23/1999)

HEC-RAS model		
Non-flooded area	Flooded area	Regular river area
62.67 [39.9%]	4.64 [3.0%]	0 [0.0%]
4.34 [2.8%]	67.09 [42.7%]	6.37 [4.1%]
0.00 [0.0%]	1.27 [0.8%]	10.58 [6.7%]
	Non-flooded area 62.67 [39.9%] 4.34 [2.8%]	Non-flooded area Flooded area 62.67 [39.9%] 4.64 [3.0%] 4.34 [2.8%] 67.09 [42.7%]

Table 4. Matched-pairs *t*-tests on the water/non-water or flooded/non-flooded boundaries derived from DEM-inundation and HEC-RAS models at three flow conditions.

(a) A regular flow condition (07/28/1999)

Water/non-water boundary	t	Þ	
On north bank	1.573	12.2%	
On south bank	1.633	10.9%	

(b) At the flood-stage and record-high flood conditions.

	e e		rd-high flood flow 0/23/1999)	
Flooded/non-flooded boundary	t	Þ	t	Þ
On north bank	1.620	11.1%	1.612	10.3%
On south bank	1.490	14.3%	1.648	10.6%

have been manually and clearly delineated by analysts, and portions of bridges and overpasses have been removed from the DEM (Figure 8). For example, streams clearly depicted by the LIDAR DEM (Figure 8a) are barely noticeable in the NED DEM (Figure 8b). Since the airborne LIDAR sensor measures surface elevation, surface elevations of bridges and overpasses will appear on the uncorrected DEM instead of that of the underlying surfaces. The hydro-correction is necessary to ensure the flow continuity of water in streams under bridges and on road surfaces beneath overpasses. Thus, because of the hydro-correction, the delineation of the center line of a steam becomes easy or may already be done; this simplifies the implementation of the DEM-inundation model (within the state of North Carolina).

The DEM-inundation model is designed to be used on a stream section between two gauging sta-

tions where preferably no major inflow from tributaries exists. With the inflow (from the tributaries into the main steam) the surface water height at the downstream gauging station will be augmented. Thus, the inflow can affect the model output. Although this may limit the applicability of the model, the ever increasing number of gauging stations in the United States is making this less of a problem. For example, in the study area, three additional gauging stations (between the Greenville and Washington stations) have been recently added (USGS NWIS 2007). The surface water heights measured at the new Chicod Creek and Tranters Creek stations (e.g., Figures 4 and 5) will help address the influence of the tributary inflows (to the Tar River) and estimation of the surface water heights at the meeting points of the Tar River/Chicod Creek and Tar River/Tranters Creek. The new gauging station (SR1565) near Grimesland at Tar River not only divides the stream

Table 5. Error matrix and classification accuracy derived from both models at sites of regular water, flooded, and non-flooded areas. The date is 23 September 1999. The area is in km².

(a) DEM-inundation model

			Reference data		
_	Model output	Flooded area	Non-flooded area	Regular water area	Total
2.	Flooded area	4.17	0.31	0.24	4.72
	Non-flooded area	0.24	4.98	0.08	5.30
	Regular water area	0.00	0.03	4.31	4.34
	Total	4.41	5.32	4.63	14.36

W	Producer's accuracy (%)	User's accuracy (%)
Flooded area	88.3	94.6
Non-flooded area	93.9	93.6
Regular water area	99.3	93.1

Overall Accuracy 95.1%

(b) HEC-RAS Model

		Reference data		
Model output	Flooded area	Non-flooded area	Regular water area	Total
Flooded area	4.22	0.23	0.18	4.63
Non-flooded area	0.19	5.04	0.06	5.29
Regular water area	0.00	0.05	4.39	4.44
Total	4.41	5.32	4.63	14.36

¥:	Producer's accuracy (%)	User's accuracy (%)	
Flooded area	91.1	95.7	
Non-flooded area	95.2	94.7	
Regular water area	98.9	94.8	

Overall Accuracy 93.1%

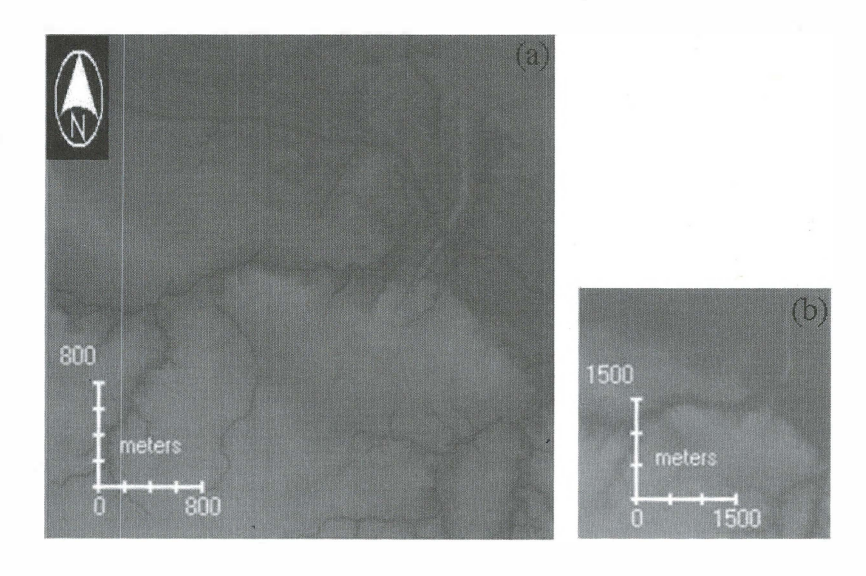


Figure 8. Streams or centerlines are clearly delineated in the hydro-corrected LIDAR DEM (a) as compared to the USGS DEM (b). The DEMs cover areas near (east of) Greenville, NC.

segment between Greenville and Washington into two segments, but also provides another independent measurement of the surface water height. Furthermore, the USGS currently maintains a network of nearly 18,000 gauging stations across the country. The high density of gauging stations has made it more likely that there is no major tributary between two stations. Finally, using real-time surface water height measurements available at gauging stations, one can use the model to simulate a range of floodextent scenarios in an event of a flood. Therefore, the DEM-inundation model will be capable of meeting the needs for quick implementation in urgent situations by the flood management and mitigation agencies at different government levels, especially in situations where there is a lack of sufficient hydrologic/hydraulic knowledge and limited resources to implement the more complex models (e.g., HEC-RAS, TELEMAC-2D, and LISFLOOD-FP).

References

Ackerman, C. T., Evans, T. A., and Brunner, G. W., 2000. HEC-GeoRAS: Linking GIS to hydraulic analysis using ARC/INFO and HEC-RAS. In: Maidment, D., Djokie, D. (Eds.), Hydrologic and Hydraulic Modeling Support with Geographic Information Systems. ESRI Press, New York.

Acrement, Jr., G., and Schneider, V., 1989. Guide for selecting Manning's roughness coefficients for natural channel and floodplains. *USGS Technical Report WSP2339*.

Al-Sabhan, W., Mulligan, M., and Blackburn, G. A., 2003. A real-time hydrologic model for flood prediction using GIS and the WWW. Computers, Environment, and Urban Systems. 27, 9-32.

Bates, P. D., and De Roo, A. P. J., 2000. A simple raster-based model for flood inundation simulation. *Journal of Hydrology*, 236, pp. 54-77.

Bates, P. D., Wilson, M. D., Horritt, M. S., 2006. Reach scale floodplain inundation dynamics observed using airborne synthetic aperture radar

- imagery: Data analysis and modeling. *Journal of Hydrology*, 328 (1-2): 306-318
- Chang, T. J., Hsu, M-H., Teng, W-H., and Huang, C-J., 2000. A GIS-assisted distributed watershed model for simulating flooding and inundation. *Journal of the American Water Resources Association*. 36(5): 975-988.
- Chow, V. T., 1959. Open Channel Hydraulies. McGraw-Hill Book Company, New York.
- Colby, J. D., Mulcahy, K., and Wang, Y., 2000. Modeling flooding extent from Hurricane Floyd in the coastal plains of North Carolina. *Environmental Hazards*. 2: 157-168.
- Correia, F. N., Rego, F. C., Saraiva, M. D., and Ramos, I., 1998. Coupling GIS with hydrologic and hydraulic flood modeling. *Water Resources Management*. 12: 229-249.
- Dobson, R., and Li, X., 2000. The accuracy and efficiency of GIS-based floodplain determinations. In: Maidment, D., Djokie, D. (Eds.), Hydrologic and Hydraulic Modeling Support with Geographic Information Systems. ESRI Press, New York.
- Galland, J. C., Goutal, N., Hervouet, J. M., 1991. TELEMAC-a new numerical-model for solving shallow-water equations. *Advances in Water Resources*. 14 (3): 138-148.
- Horritt, M. S., and Bates, P. D., 2001. Effects of spatial resolution on a raster based model of flood flow. *Journal of Hydrology*. 253, pp. 239-249.
- Horritt, M. S., and Bates, P. D., 2002. Evaluation of 1D and 2D numerical models for predicting river flood inundation. *Hydrological Processes*. 268 (1-4): 87-99 NOV 1 2002.
- Horritt, M. S., Bates, P. D., and Mattinson, M. J., 2006. Effects of mesh resolution and topographic representation in 2D finite volume models of shallow water fluvial flow. *Journal of Hydrology*. 329 (1-2): 306-314.
- Hunter, N. M., Bates, P. D., Horritt, M. S., De Roo, P. J., and Werner, M. G. F., 2005. Utility of different data types for calibrating flood inundation models within a GLUE framework. *Hydrology and Earth System Sciences.* 9 (4): 412-430.
- Hydraulic Engineering Center, 1997. HEC-RAS River Analysis system: Hydraulic Reference Manual. Hydraulic Engineering Center, Davis, CA.

- Kraus, R., 2000. Floodplain determination using ArcView GIS and HEC-RAS. In: Maidment, D., Djokie, D. (Eds.), Hydrologic and Hydraulic Modeling Support with Geographic Information Systems. ESRI Press, New York.
- Mileti, D. S., 1999. Disasters by design: a reassessment of natural hazards in the United States. John Henry Press, Washington D.C.
- NC Floodplain Mapping Program, http://www.ncfloodmaps.com. Last accessed: December 2007.
- Nicholas, A.P., and Mitchell, C.A., 2003. Numerical simulation of overbank processes in topographically complex floodplain environments. Hydrological Processes. 17 (4): 727-746.
- USACE, http://www.hec.usace.army.mil/software/hec-ras/. Last Accessed: December 2007.
- USGS NED, http://ned.usgs.gov/. Last accessed: December 2007.
- USGS NWIS, http://waterdata.usgs.gov/nc/nwis. Last accessed: December 2007.
- Wang, Y., Colby, J., and Mulcahy, K., 2002. An efficient method for mapping flood extent in a coastal floodplain by integrating Landsat TM and DEM data. *International Journal of Remote Sensing*. 23(18) 3681-3696.
- Wang, Y., 2004. Using Landsat 7 TM data acquired days after a flood event to delineate the maximum flood on a coastal floodplain. *International Journal of Remote Sensing*, 25(5) 959-974.
- Wang, Y. and Zheng, T., 2005. Comparison of digital elevation models and understanding of their impact on the flood extent mapping on a coastal floodplain of North Carolina, *Natural Hazards Review*, 6(1), 34-40.
- Werner, M. G. F., 2001. Impact of grid size in GIS based flood extent mapping using a 1-D flow model. *Physics and Chemistry of the Earth Part B-Hydrology Oceans and Atmosphere*. 26, pp. 517-522.
- Werner M. G. F., Hunter, N. M., Bates, P. D., 2005. Identifiability of distributed floodplain roughness values in flood extent estimation. *Journal of Hydrology*. 314 (1-4): 139-157.
- Wilson, C., and Horritt, M., 2002. Measuring the flow resistance of submerged grass. *Hydrological Processes*. 16, 2589-2598.

- Wilson, C. A., M. E., Stoesser, T., Bates, P. D., and Batemann Pinzen, A., 2006. Closure to "Open channel flow through different forms of submerged flexible vegetation". *Journal of Hydraulic Engineering-ASCE*. 132 (7): 750-750.
- Yang, C., and Tsai, C., 2000. Development of a GIS-based flood information system for flood-plain modeling and damage calculation. *Journal of the American Water Resources Association*. 36 (3): 567-577.